Proceedings of the 26th International Conference on Offshore Mechanics and Arctic Engineering
OMAE2007
June 10-15, 2007, San Diego, California, USA

OMAE2007-29314

HAMILTONIAN FORMULATION AND LONG WAVE MODELS FOR INTERNAL WAVES

Walter Craig
Department of Mathematics
McMaster University
Hamilton, ON L8S 4K1, Canada
Email: craig@math.mcmaster.ca

Philippe Guyenne*
Department of Mathematics
University of Delaware
Newark, DE 19716
Email: guyenne@math.udel.edu

Henrik Kalisch
Department of Mathematics
University of Bergen
5008 Bergen, Norway
Email: henrik.kalisch@math.uib.no

ABSTRACT

We derive a Hamiltonian formulation of the problem of a dynamic free interface (with rigid lid upper boundary conditions), and of a free interface coupled with a free surface, this latter situation occurring more commonly in experiment and in nature. Based on the linearized equations, we highlight the discrepancies between the cases of rigid lid and free surface upper boundary conditions, which in some circumstances can be significant. We also derive systems of nonlinear dispersive long wave equations in the large amplitude regime, and compute solitary wave solutions of these equations.

INTRODUCTION

Internal waves in a fluid body occur in a sharp interface between two fluids of different densities. Scientific interest in internal waves includes the need to quantify induced loads on submerged engineering constructions (such as oil platforms and rail and road tunnels lying on the sea bed), as well as the mathematical interest in the variety of nonlinear dispersive evolution equations that occur in the discipline of free surface hydrodynamics. In nature they are observed in the pycnocline induced by an abrupt jump in salinity, often occurring in fjords, and in thermoclines found in relatively common situations in tropical seas. Observations report amplitudes of internal waves greater than 100m in fluid bodies of depth less than 1000m with wavelength of one to ten kilometers. This is a highly nonlinear regime of wave motion, characterized by large amplitudes which are nevertheless of small slope. Additionally, in oceanographic observations, waves on the sea surface are affected in a nontrivial manner by the presence of disturbances in the interface. Indeed one characteristic signature of internal waves can be a change in the smaller scale wave patterns in the surface, giving rise to a differential reflectancy property under oblique lighting. We are also motivated by the recent work of Choi and Camassa [1] on internal waves, and their models for larger amplitude long wave motion.

In this paper we give a formulation for the equations of motion of a system of one or several ideal fluids with a dynamic free surface, free interfaces, or both, as Hamiltonian systems with infinitely many degrees of freedom. The top surface of the upper layer is either subject to rigid lid boundary conditions, or else it is itself a free surface. We confine our considerations to two dimensional fluid motions, which are valid approximations for long-crested waves. In principle our methods extend to the fully three dimensional case. A Hamiltonian formulation of the problem of a free interface between two ideal fluids, under rigid lid boundary conditions for the upper fluid, was given by Benjamin and Bridges [2]. Craig and Groves [3] gave a similar expression for Benjamin and Bridges' Hamiltonian for the free interface problem, using the Dirichlet-Neumann operators for both the upper and lower fluid domains. Our present formulation of the problem is complete, with the Hamiltonian being given in terms of the deformations of the free surface and the free interface, the traces of the velocity potential functions on them, and the Dirichlet-Neumann operators for the upper and lower fluid domains. This formulation has implications for the convenience of perturbation calculations in these variables.

We focus here on quantifying the difference between the

*Address all correspondence to this author.

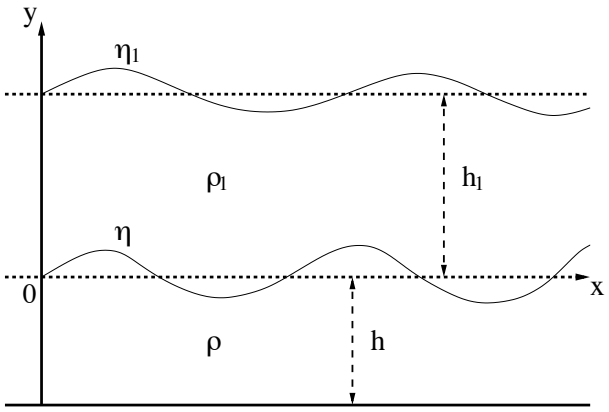

Figure 1. Sketch of the physical problem.

choice of rigid lid boundary conditions, most often used in mathematical modeling, and the setting of a free surface top boundary, which is the physically most relevant case. There are a number of important differences, affecting in particular the linear dispersion relation and the linear wave speed. In addition we develop new model systems of equations for perturbation regimes in which wave profiles have small slope, but with amplitudes that are fully of the same order as the mean depth of the fluid layers. This regime reflects the realities of the observed interfacial waves in the ocean, where the ratio of amplitude to layer depth may be of order $O(1)$, while the ratio of amplitude to wavelength remains small. In this scaling regime, we have found unusual and interesting Hamiltonian models which have nonlinear rational coefficients of dispersion. These models admit solitary wave solutions which are computed numerically and compared with other existing models.

This paper is structured as follows. In the next section, we derive the Hamiltonian formulation of the free interface problem and the problem of a free surface above a free interface, using the description of the Dirichlet integral for the velocity potentials in terms of the Dirichlet-Neumann operators on the fluid domain boundaries. This is followed by the analysis of two linearized problems; the free interface case with rigid lid boundary conditions on the upper surface, and the free interface with free surface boundary conditions on the upper fluid surface. We quantify the behavior of the dispersion relations of the two problems, and indicate a number of significant differences. We then study the long wave regime for the free interface problem with an upper rigid lid. We describe the setting of large interfacial deviations of small slope, between finite upper and lower layers. Numerical results on solitary wave solutions are shown.

Most of the results presented here have been described in [4–6]. New computations of internal solitary waves in certain parameter regimes are shown (Fig. 4).

EQUATIONS OF MOTION

The fluid domain is the region consisting of the points (x,y) such that $-h<y<h_1+\eta_1(x,t)$, and it is divided into two regions $S(t;\eta)=\{(x,y):-h<y<\eta(x,t)\}$ and $S_1(t;\eta,\eta_1)=\{(x,y):\eta(x,t)<y<h_1+\eta_1(x,t)\}$ by the interface $\{y=\eta(x,t)\}$. The two regions are occupied by two immiscible fluids, with ρ the density of the lower fluid and ρ_1 the density of the upper fluid (Fig. 1). The system is in a stable configuration, in that $\rho>\rho_1$. In such a configuration, the fluid motion is assumed to be potential flow, namely in Eulerian coordinates the velocity is given by a potential in each fluid region, $\mathbf{u}(x,y,t)=\nabla\varphi(x,y,t)$ in $S(t;\eta)$, and $\mathbf{u}_1(x,y,t)=\nabla\varphi_1(x,y,t)$ in $S_1(t;\eta,\eta_1)$, where the two potential functions satisfy

$$\begin{aligned}\Delta\varphi &= 0\,, \quad \text{in the domain } S(t;\eta)\\ \Delta\varphi_1 &= 0\,, \quad \text{in the domain } S_1(t;\eta,\eta_1)\,.\end{aligned} \tag{1}$$

The boundary conditions on the fixed bottom $\{y=-h\}$ of the lower fluid are that

$$\nabla\varphi\cdot N_0(x,-h)=-\partial_y\varphi(x,-h)=0\,, \tag{2}$$

where N_0 is the exterior unit normal, enforcing that there is no fluid flux across the boundary.

On the interface $\{(x,y):y=\eta(x,t)\}$ it is natural to impose three boundary conditions, two kinematic conditions which are essentially geometrical, and a physical condition of force balance. The kinematical conditions assume that there is no cavitation in the interface between the fluids, and therefore the function $\eta(x,t)$ whose graph defines the interface satisfies simultaneously

$$\partial_t\eta=\partial_y\varphi-\partial_x\eta\,\partial_x\varphi=\nabla\varphi\cdot N(1+|\partial_x\eta|^2)^{1/2} \tag{3}$$

where N is the unit exterior normal on the interface for the lower domain, and

$$\partial_t\eta=\partial_y\varphi_1-\partial_x\eta\,\partial_x\varphi_1=-\nabla\varphi_1\cdot(-N)(1+|\partial_x\eta|^2)^{1/2}\,. \tag{4}$$

The third boundary condition imposed on the interface is the Bernoulli condition, which states that

$$\rho(\partial_t\varphi+\tfrac{1}{2}|\nabla\varphi|^2+g\eta)=\rho_1(\partial_t\varphi_1+\tfrac{1}{2}|\nabla\varphi_1|^2+g\eta)\,. \tag{5}$$

Finally, in assigning boundary conditions for the upper boundary in the problem, we are interested in considering two situations. The first is where $\eta_1=0$ and the top surface is considered a solid boundary (a rigid lid). In this case the boundary

condition

$$\nabla\varphi_1 \cdot N_1(x,h_1) = \partial_y\varphi_1(x,h_1) = 0 \tag{6}$$

is appropriate, where N_1 is the unit exterior normal to the upper fixed surface. The problem is therefore to find the evolution of a single free interface $\{(x,\eta(x,t))\}$. We allow $0 < h, h_1 \leq +\infty$, and either h or h_1 or both are specifically allowed to be infinite.

The second situation that we consider is where the top surface is itself a free surface $\{(x,y) : y = h_1 + \eta_1(x,t)\}$, on which the velocity potential φ_1 and the function η_1 satisfy a surface kinematic condition

$$\partial_t\eta_1 = \partial_y\varphi_1 - \partial_x\eta_1\,\partial_x\varphi_1 = \nabla\varphi_1 \cdot N_1(1+|\partial_x\eta_1|^2)^{1/2} \tag{7}$$

and a Bernoulli condition

$$\partial_t\varphi_1 + \tfrac{1}{2}|\nabla\varphi_1|^2 + g\eta_1 = 0\,. \tag{8}$$

The problem then is to describe the simultaneous evolution of the free surface $\{(x,h_1+\eta_1(x,t))\}$ and the free interface $\{(x,\eta(x,t))\}$.

HAMILTONIAN FORMULATION AND DIRICHLET-NEUMANN OPERATOR

Hamiltonian for Free Interfaces

It is straightforward to derive useful expressions for the kinetic energy and the potential energy for the first system above, consisting of one free interface separating two otherwise confined fluid regions. From these one can pose a Lagrangian for the system. In an analogy with classical mechanics the Hamiltonian for the system and the form of the canonically conjugate variables can be derived. In this way we deduce from the 'first principles' of mechanics the form of the canonical variables that were originally given in Benjamin and Bridges [2].

The kinetic energy is given by the weighted sum of Dirichlet integrals of the two velocity potentials,

$$\begin{aligned} K = {} & \tfrac{1}{2}\int_{\mathbb{R}}\int_{-h}^{\eta(x)} \rho|\nabla\varphi(x,y)|^2\,dydx \\ & + \tfrac{1}{2}\int_{\mathbb{R}}\int_{\eta(x)}^{h_1} \rho_1|\nabla\varphi_1(x,y)|^2\,dydx\,, \end{aligned} \tag{9}$$

and the potential energy is

$$\begin{aligned} V &= \int_{\mathbb{R}}\int_{-h}^{\eta(x)} g\rho y\,dydx + \int_{\mathbb{R}}\int_{\eta(x)}^{h_1} g\rho_1 y\,dydx \\ &= \tfrac{1}{2}\int_{\mathbb{R}} g\rho\eta^2(x)\,dx - \tfrac{1}{2}\int_{\mathbb{R}} g\rho_1\eta^2(x)\,dx + C\,. \end{aligned} \tag{10}$$

The constant term C is superfluous to the dynamics, and it is able to be normalized to zero. Following the analogy with mechanics, the Lagrangian of the system is given by $L = K - V$.

To place the kinetic energy in a more convenient expression for analysis, we introduce the Dirichlet-Neumann operators for the two fluid domains. Let N be the unit exterior normal to the lower fluid domain $S(\eta)$ along the free interface. Given $\Phi(x) = \varphi(x,\eta(x))$ and $\Phi_1(x) = \varphi_1(x,\eta(x))$ the boundary values of the two velocity potentials on the free interface $\{(x,\eta(x,t))\}$, and following Craig and Sulem [7], define the operators

$$G(\eta)\Phi = \nabla\varphi \cdot N(1+|\partial_x\eta|^2)^{1/2}\,, \tag{11}$$

which is the Dirichlet-Neumann operator for the fluid domain $S(\eta)$, and

$$G_1(\eta)\Phi_1 = -\nabla\varphi_1 \cdot N(1+|\partial_x\eta|^2)^{1/2}\,, \tag{12}$$

the Dirichlet-Neumann operator for the fluid domain $S_1(\eta)$. These operators are linear in the quantities Φ and Φ_1, however they are nonlinear and reasonably complicated in their dependence on $\eta(x)$ which determines the two fluid domains. Using Green's identities, the kinetic energy (9) can be rewritten as

$$K = \tfrac{1}{2}\int_{\mathbb{R}} \rho\Phi G(\eta)\Phi\,dx + \tfrac{1}{2}\int_{\mathbb{R}} \rho_1\Phi_1 G_1(\eta)\Phi_1\,dx\,. \tag{13}$$

Under the conditions of no cavitation at the interface, the kinetic boundary conditions (3)-(4) read

$$\partial_t\eta = G(\eta)\Phi = -G_1(\eta)\Phi_1\,. \tag{14}$$

Solving (14) for $\Phi(x) = G^{-1}(\eta)\dot\eta(x)$ and $\Phi_1(x) = -G_1^{-1}(\eta)\dot\eta(x)$ and substituting into the quantity (13) one obtains a reasonable expression for the Lagrangian

$$\begin{aligned} L(\eta,\dot\eta) = {} & \tfrac{1}{2}\int_{\mathbb{R}} \rho\dot\eta G^{-1}(\eta)\dot\eta + \rho_1\dot\eta G_1^{-1}(\eta)\dot\eta\,dx \\ & - \tfrac{1}{2}\int_{\mathbb{R}} g(\rho-\rho_1)\eta^2(x)\,dx\,. \end{aligned}$$

From this Lagrangian, which depends upon $(\eta,\dot\eta)$, we are in a position to deduce from the principles of classical mechanics the Hamiltonian and the canonically conjugate variables with respect to which the system (1)-(6) is formally a Hamiltonian dynamical system. Namely, we define

$$\begin{aligned} \xi(x) &= \delta_{\dot\eta}L = \rho G^{-1}(\eta)\dot\eta + \rho_1 G_1^{-1}\dot\eta \\ &= \rho\Phi(x) - \rho_1\Phi_1(x)\,, \end{aligned} \tag{15}$$

which is precisely the expression of Benjamin and Bridges [2] for the variable conjugate to $\eta(x)$.

The Hamiltonian for the system is given by $K+V$ since L is a quadratic form in $\dot{\eta}$. Using (14) and (15), one finds that $(\rho_1 G(\eta)+\rho G_1(\eta))\Phi = G_1(\eta)\xi$ and $(\rho G_1(\eta)+\rho_1 G(\eta))\Phi_1 = -G(\eta)\xi$, whereupon the Hamiltonian can be written

$$H(\eta,\xi) = \tfrac{1}{2}\int_{\mathbb{R}} \xi G_1(\eta)(\rho_1 G(\eta)+\rho G_1(\eta))^{-1} G(\eta)\xi\, dx + \tfrac{1}{2}\int_{\mathbb{R}} g(\rho-\rho_1)\eta^2\, dx\,. \tag{16}$$

This expression for the Hamiltonian has appeared in [3]. The system of equations of motion for the interface takes the form of a classical Hamiltonian system, namely

$$\partial_t \eta = \delta_\xi H\,, \qquad \partial_t \xi = -\delta_\eta H\,, \tag{17}$$

which is equivalent to (1) subject to the boundary conditions (2), (6) and the free interface conditions (3)-(5). Expressions for $G(\eta)$ and $G_1(\eta)$ can be found in [3, 7].

We note that by setting $\rho_1 = 0$ the expressions (10) and (13) reduce to the ones for a single free surface alone, the canonical conjugate variables (15) state that $\xi(x) = \rho\Phi(x)$ which is precisely the choice of Zakharov [8], and the sum $K+V$ is the Hamiltonian for the system.

Hamiltonian for Free Surfaces and Interfaces

In the second situation described above, the system of interest involves the coupled evolution of the free interface and a free surface lying over the upper fluid. This problem can also be described in terms of a Lagrangian, which will depend upon both the deformations $\eta_1(x,t)$ of the free surface, as well as those of the free interface $\eta(x,t)$. Again the 'first principles' of mechanics can be cited in deriving the natural canonically conjugate variables for a Hamiltonian description of the problem, and for a convenient expression for the Hamiltonian function. This choice of variables has been previously given by Ambrosi [9], however the form of the Hamiltonian is to our knowledge new.

As in the first case, the kinetic energy is again given as a weighted sum of the Dirichlet integrals of the two velocity potentials, namely

$$K = \tfrac{1}{2}\int_{\mathbb{R}}\int_{-h}^{\eta(x)} \rho|\nabla\varphi(x,y)|^2\, dy dx + \tfrac{1}{2}\int_{\mathbb{R}}\int_{\eta(x)}^{h_1+\eta_1(x)} \rho_1|\nabla\varphi_1(x,y)|^2\, dy dx\,. \tag{18}$$

In a manner similar to (10), the potential energy is

$$V = \tfrac{1}{2}\int_{\mathbb{R}} g(\rho-\rho_1)\eta^2(x)\, dx + \tfrac{1}{2}\int_{\mathbb{R}} g\rho_1\eta_1^2(x) + 2g\rho_1 h_1\eta_1(x)\, dx + C\,. \tag{19}$$

The analogy with mechanics implies that the Lagrangian of the system is given by $L = K - V$.

Following (13), we express the Dirichlet integrals in terms of the boundary values for the two velocity potentials and the Dirichlet-Neumann operators for the two fluid domains. We define the quantities $\Phi(x) = \varphi(x,\eta(x))$, $\Phi_1(x) = \varphi_1(x,\eta(x))$ as above, and $\Phi_2(x) = \varphi_1(x, h_1+\eta_1(x))$ on the free surface. The Dirichlet-Neumann operator for the lower domain is the same as in the first case, namely $G(\eta)\Phi(x) = \nabla\varphi\cdot N(1+(\partial_x\eta)^2)^{1/2}$. For the upper fluid domain $S_1(\eta,\eta_1)$ both $\Phi_1(x)$ and $\Phi_2(x)$ contribute to the exterior unit normal derivative of φ_1 on each boundary. That is, the Dirichlet-Neumann operator is a matrix operator which takes the form

$$\begin{pmatrix} G_{11} & G_{12} \\ G_{21} & G_{22}\end{pmatrix}\begin{pmatrix}\Phi_1(x)\\ \Phi_2(x)\end{pmatrix} = \begin{pmatrix} -(\nabla\varphi_1\cdot N)(x,\eta(x))(1+(\partial_x\eta(x))^2)^{1/2} \\ (\nabla\varphi_1\cdot N_1)(x,h_1+\eta_1(x))(1+(\partial_x\eta_1(x))^2)^{1/2}\end{pmatrix}\,. \tag{20}$$

Using Green's identities, and expressing the normal derivatives of the velocity potentials on the boundaries in terms of Dirichlet-Neumann operators, the kinetic energy takes the form

$$K = \tfrac{1}{2}\int_{\mathbb{R}} \rho\Phi G(\eta)\Phi\, dx + \tfrac{1}{2}\int_{\mathbb{R}} \rho_1 \begin{pmatrix}\Phi_1\\ \Phi_2\end{pmatrix}^T \begin{pmatrix} G_{11} & G_{12}\\ G_{21} & G_{22}\end{pmatrix}\begin{pmatrix}\Phi_1\\ \Phi_2\end{pmatrix} dx\,. \tag{21}$$

In terms of the Dirichlet-Neumann operators (11)(20), the kinematic boundary condition (14) for $\Phi(x)$ is unchanged, while (4) and (7) become

$$\begin{aligned}\dot{\eta} &= -(G_{11}\Phi_1 + G_{12}\Phi_2)\\ \dot{\eta}_1 &= G_{21}\Phi_1 + G_{22}\Phi_2\,.\end{aligned} \tag{22}$$

Using (14) and (22) we rewrite the kinetic energy in terms of the variables $(\eta,\eta_1,\dot{\eta},\dot{\eta}_1)$, giving the following expression for the Lagrangian for the free surface/free interface problem;

$$\begin{aligned} L = {} & \tfrac{1}{2}\int_{\mathbb{R}} \rho\dot{\eta}G^{-1}(\eta)\dot{\eta}\, dx \\ & + \tfrac{1}{2}\int_{\mathbb{R}} \rho_1 \begin{pmatrix}-\dot{\eta}\\ \dot{\eta}_1\end{pmatrix}^T \begin{pmatrix} G_{11} & G_{12}\\ G_{21} & G_{22}\end{pmatrix}^{-1}\begin{pmatrix}-\dot{\eta}\\ \dot{\eta}_1\end{pmatrix} dx \\ & - \tfrac{1}{2}\int_{\mathbb{R}} g(\rho-\rho_1)\eta^2(x)\, dx - \tfrac{1}{2}\int_{\mathbb{R}} g\rho_1(h_1+\eta_1)^2(x)\, dx\,. \end{aligned} \tag{23}$$

In these terms we are able to deduce from 'first principles' the appropriate canonically conjugate variables for the problem, namely

$$\begin{pmatrix}\xi\\ \xi_1\end{pmatrix} = \begin{pmatrix}\delta_{\dot\eta}L\\ \delta_{\dot\eta_1}L\end{pmatrix} = \rho\begin{pmatrix}G^{-1}(\eta)\dot\eta\\ 0\end{pmatrix} + \rho_1\begin{pmatrix}G_{11} & -G_{12}\\ -G_{21} & G_{22}\end{pmatrix}^{-1}\begin{pmatrix}\dot\eta\\ \dot\eta_1\end{pmatrix} = \begin{pmatrix}\rho\Phi - \rho_1\Phi_1\\ \rho_1\Phi_2\end{pmatrix} . \tag{24}$$

The expression (24) also appears in [9]. Using (24), the kinetic energy (21) has the form

$$K = \tfrac{1}{2}\int_{\mathbb{R}}\begin{pmatrix}\xi\\ \xi_1\end{pmatrix}^T\begin{pmatrix}\dot\eta\\ \dot\eta_1\end{pmatrix}dx = \tfrac{1}{2}\int_{\mathbb{R}}\begin{pmatrix}\xi\\ \xi_1\end{pmatrix}^T\begin{pmatrix}-G_{11} & -G_{12}\\ G_{21} & G_{22}\end{pmatrix}\begin{pmatrix}\Phi_1\\ \Phi_2\end{pmatrix}dx . \tag{25}$$

Solving (14) and (24) for (Φ,Φ_1,Φ_2) in terms of (ξ,ξ_1), and defining $\rho G_{11}+\rho_1 G(\eta) = B$, we have

$$\begin{aligned}\Phi &= B^{-1}(G_{11}\xi - G_{12}\xi_1)\\ \Phi_1 &= B^{-1}\left(-G(\eta)\xi - \frac{\rho}{\rho_1}G_{12}\xi_1\right)\\ \rho_1\Phi_2 &= \xi_1 ,\end{aligned} \tag{26}$$

and (25) can be written as

$$K = \tfrac{1}{2}\int_{\mathbb{R}}\begin{pmatrix}\xi\\ \xi_1\end{pmatrix}^T\begin{pmatrix}G_{11}B^{-1}G(\eta) & -G(\eta)B^{-1}G_{12}\\ -G_{21}B^{-1}G(\eta) & \frac{1}{\rho_1}G_{22} - \frac{\rho}{\rho_1}G_{21}B^{-1}G_{12}\end{pmatrix}\times\begin{pmatrix}\xi\\ \xi_1\end{pmatrix}dx . \tag{27}$$

The Hamiltonian for the free surface and free interface problem is $H = K+V$ where $K = K(\eta,\eta_1,\xi,\xi_1)$ is given by (27) and the potential energy $V = V(\eta,\eta_1)$ is simply (19). This expression corrects [9] in giving the full coupling in the kinetic energy between the variables ξ and ξ_1. Expressions for the G_{ij} can be found in [5]. Hamilton's equations of motion take the form

$$\begin{aligned}\partial_t\eta &= \delta_\xi H , \qquad \partial_t\xi = -\delta_\eta H ,\\ \partial_t\eta_1 &= \delta_{\xi_1}H , \qquad \partial_t\xi_1 = -\delta_{\eta_1}H ,\end{aligned} \tag{28}$$

for the interface and free surface respectively.

LINEARIZED EQUATIONS

Linear Free Interfaces

Restricting to the quadratic part of the Hamiltonian (16), one obtains

$$H = \frac{1}{2}\int_{\mathbb{R}}\left[\xi\frac{D\tanh(hD)\tanh(h_1D)}{\rho\tanh(h_1D)+\rho_1\tanh(hD)}\xi + g(\rho-\rho_1)\eta^2\right]dx , \tag{29}$$

where $D = -i\partial_x$. The linearized form of (17) then reads

$$\begin{aligned}\partial_t\eta &= \delta_\xi H = \frac{D\tanh(hD)\tanh(h_1D)}{\rho\tanh(h_1D)+\rho_1\tanh(hD)}\xi ,\\ \partial_t\xi &= -\delta_\eta H = -g(\rho-\rho_1)\eta .\end{aligned} \tag{30}$$

The corresponding dispersion relation giving the wave frequency $\omega(k)$ as a function of the wavenumber k is

$$\omega^2 = \frac{g(\rho-\rho_1)k\tanh(kh)\tanh(kh_1)}{\rho\tanh(kh_1)+\rho_1\tanh(kh)} . \tag{31}$$

Equivalently, it can be stated in terms of the phase velocity of a single Fourier mode

$$c = \frac{\omega}{k} = \sqrt{\frac{g(\rho-\rho_1)\tanh(kh)\tanh(kh_1)}{k(\rho\tanh(kh_1)+\rho_1\tanh(kh))}} . \tag{32}$$

In the long-wave regime, we can distinguish three different situations giving rise to characteristic asymptotics for the phase speed (32); the first being where both $kh\to 0$ and $kh_1\to 0$ (two finite layers), with the ratio h_1/h fixed,

$$c^2 \simeq c_0^2 = \frac{g(\rho-\rho_1)}{\rho/h+\rho_1/h_1} . \tag{33}$$

The second is where $kh > O(1)$ (deep lower layer) while $kh_1\to 0$ (finite upper layer) (or the reverse situation in which $kh\to 0$ while $kh_1 > O(1)$). Then

$$c^2 \simeq c_0^2 = g\frac{\rho-\rho_1}{\rho_1/h_1} \tag{34}$$

(respectively, $c_0^2 = g(\rho-\rho_1)/(\rho/h)$). The third situation occurs for two deep layers separated by the free interface. Letting $k\to 0$ while both kh and $kh_1 > O(1)$, one finds

$$\omega_0^2 = \frac{g(\rho-\rho_1)}{\rho+\rho_1}k . \tag{35}$$

In the opposite regime, one lets $k \to +\infty$ while fixing the fluid domain geometry. The resulting asymptotic behavior of the dispersion relation is that

$$\omega_\infty^2 = \frac{g(\rho-\rho_1)}{\rho+\rho_1}k\,, \tag{36}$$

which coincides with the scaling invariant third situation above. These expressions are to be compared with the case of a free surface lying over a free interface in a two fluid system.

Linear Free Surfaces and Interfaces

Using (19) and (27), the quadratic part of the Hamiltonian for the problem of a free interface underlying a free surface is given by

$$\begin{aligned} H = \frac{1}{2}\int_{\mathbb{R}} \Big[& \xi \frac{D\tanh(hD)\coth(h_1D)}{\rho\coth(h_1D)+\rho_1\tanh(hD)}\xi \\ & + 2\xi \frac{D\tanh(hD)\operatorname{csch}(h_1D)}{\rho\coth(h_1D)+\rho_1\tanh(hD)}\xi_1 \\ & + \xi_1 \frac{D(\coth(h_1D)\tanh(hD)+(\rho/\rho_1))}{\rho\coth(h_1D)+\rho_1\tanh(hD)}\xi_1 \\ & + g(\rho-\rho_1)\eta^2 + g\rho_1\eta_1^2\Big]dx\,. \end{aligned} \tag{37}$$

The linearized equations of motion are

$$\begin{aligned} \partial_t\eta = \delta_\xi H &= \frac{D\tanh(hD)\coth(h_1D)}{\rho\coth(h_1D)+\rho_1\tanh(hD)}\xi \\ &\quad + \frac{D\tanh(hD)\operatorname{csch}(h_1D)}{\rho\coth(h_1D)+\rho_1\tanh(hD)}\xi_1 \\ \partial_t\xi = -\delta_\eta H &= -g(\rho-\rho_1)\eta\,, \end{aligned}$$

and

$$\begin{aligned} \partial_t\eta_1 = \delta_{\xi_1} H &= \frac{D\tanh(hD)\operatorname{csch}(h_1D)}{\rho\coth(h_1D)+\rho_1\tanh(hD)}\xi \\ &\quad + \frac{D(\coth(h_1D)\tanh(hD)+(\rho/\rho_1))}{\rho\coth(h_1D)+\rho_1\tanh(hD)}\xi_1 \\ \partial_t\xi_1 = -\delta_{\eta_1} H &= -g\rho_1\eta_1\,. \end{aligned} \tag{38}$$

The corresponding dispersion relation for ω^2 is determined by the quadratic equation

$$\begin{aligned} \omega^4 - g\rho k\frac{1+\tanh(kh)\coth(kh_1)}{\rho\coth(kh_1)+\rho_1\tanh(kh)}\omega^2 \\ + g^2(\rho-\rho_1)k^2\frac{\tanh(kh)}{\rho\coth(kh_1)+\rho_1\tanh(kh)} = 0\,. \end{aligned} \tag{39}$$

The two solutions $\omega^\pm(k)$ of (39) are associated with two different modes of wave motion, namely surface and interface displacements. They are given by

$$\begin{aligned} (\omega^\pm)^2 = & \frac{1}{2}g\rho k\frac{1+\tanh(hk)\coth(h_1k)}{\rho\coth(h_1k)+\rho_1\tanh(hk)} \\ & \pm\frac{1}{2}gk\Big[\rho^2(1-\tanh(hk)\coth(h_1k))^2 \\ & \quad + 4\rho\rho_1\tanh(hk)(\coth(h_1k)-\tanh(hk)) \\ & \quad + 4\rho_1^2\tanh(hk)^2\Big]^{1/2} \\ & /(\rho\coth(h_1k)+\rho_1\tanh(hk))\,. \end{aligned} \tag{40}$$

The radicand is always positive, as can be assured by the fact that for all wavenumbers $k>0$, $\tanh(hk)<1<\coth(h_1k)$. The branch ω^+ is associated with free surface wave motion, while the linear behavior of the interface is governed by ω^- (at least in the limit of large k). This expression also appears in [10].

Comparison With the Rigid Lid Case

It is important to compare the dispersion relation ω^- for the interfacial mode with the dispersion relation ω for the case with a rigid lid (31). In the regime where $k\to+\infty$, fixing other aspects of the fluid domain, one finds that

$$(\omega_\infty^+)^2 = gk\,, \qquad (\omega_\infty^-)^2 = \frac{g(\rho-\rho_1)}{\rho+\rho_1}k\,. \tag{41}$$

The latter agrees with the asymptotics as $k\to+\infty$ of the dispersion relation (36) of the case with a rigid lid. The expression for $(\omega_\infty^+)^2 = gk$ agrees with the dynamics of the free surface with no free interface present.

However the behavior of the dispersion relations for long wave regimes are very different when considering the case of a free surface lying over a free interface and the case of rigid lid upper boundary conditions. Letting kh and $kh_1\to 0$ while fixing the ratio h/h_1 to be finite, one finds that the two phase speeds associated with the two branches of the dispersion curve $\omega^\pm$ are asymptotic to

$$(c_0^\pm)^2 = \tfrac{1}{2}g\left(h+h_1\pm\sqrt{(h-h_1)^2+4(\rho_1/\rho)hh_1}\right)\,. \tag{42}$$

We only consider $\rho_1<\rho$, so the 'faster' free surface phase velocity c_0^+ is somewhat slower than if there were no interface present. Note that the phase velocity $(c_0^-)^2$ associated with the free interface (the 'slower' dispersion curve) is positive for $\rho>\rho_1$ (stable stratification). Examining c_0^- we conclude that it can behave completely differently than the case of the rigid lid, given in (33).

There is also a significant difference between the dispersive behavior in this long wave regime, in the case of a free surface and a free interface, as compared to the case of a rigid lid.

In other situations, such as when $kh \to \infty$ (infinitely deep lower layer) and $kh_1 \to 0$ (finite upper layer),

$$(c_0^+)^2 = \frac{g}{k} \qquad \text{and} \qquad (c_0^-)^2 = gh_1\left(1-\frac{\rho_1}{\rho}\right). \tag{43}$$

This differs from the regime of two finite layers where both $(c_0^\pm)^2$ are of the same order of magnitude, as shown in (42).

In Fig. 2, we plot the linear phase speeds for the different configurations as functions of the wavenumber. The linear phase speed $c = \omega/k$ for the interface in the rigid lid case is given by (32), while those of the coupled system are given by (40) ($c^\pm = \omega^\pm/k$). We show the comparison between c and $c^\pm$ for two different values of the density ratio $\rho_1/\rho = 0.2, 0.8$ and for three different values of the depth ratio $h_1/h = 10, 1, 0.1$. As expected, c^- coincides with c at large k and their graphs always lie below that of c^+. The differences between c and c^- are most significant for small values of ρ_1/ρ. Also, the values of c and c^- are slightly larger for small ρ_1/ρ than large ρ_1/ρ. This is the fact that interfacial waves propagate more rapidly beneath a less dense fluid. For a given value of ρ_1/ρ, the differences between c and c^- are most important when the ratio h_1/h is small. When h_1/h is large, their graphs match perfectly since in this case the effects of a rigid lid or a free surface are negligible.

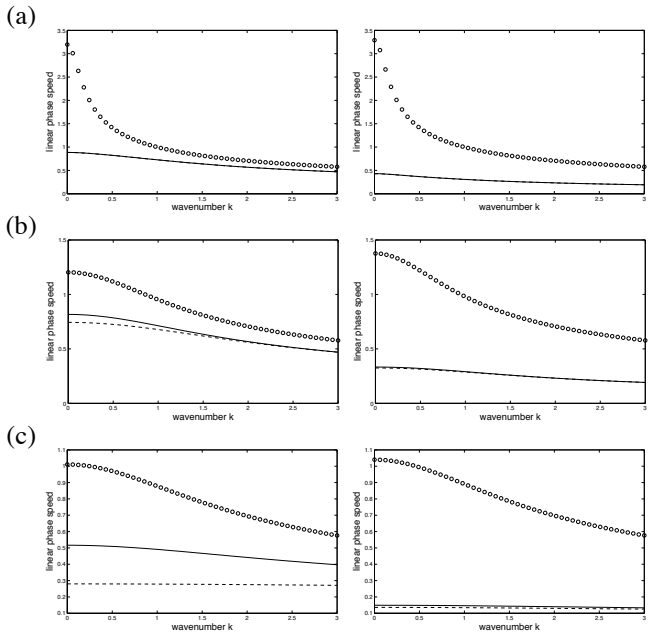

Figure 2. Linear phase speed c vs. wavenumber k for (left column) $\rho_1/\rho = 0.2$ and (right column) $\rho_1/\rho = 0.8$: (a) $h_1/h = 10$, (b) $h_1/h = 1$, (c) $h_1/h = 0.1$. The linear phase speed for the interface in the rigid lid case is represented in solid line. The linear phase speeds c^- and c^+ in the coupled system are represented in dashed line and circles respectively.

LONG WAVE MODELS

Large-Amplitude Long Internal Waves

We focus on the regime in which the typical wavelength λ of the internal waves is long compared to the depths h and h_1 of the two layers, with rigid lid boundary conditions. However the typical wave amplitude a is not assumed to be small compared to h or h_1 unlike the classical Boussinesq regime. In the framework of Hamiltonian perturbation theory, we take the small parameter to be $\varepsilon^2 \simeq (h/\lambda)^2 \simeq (h_1/\lambda)^2 \simeq (a/\lambda)^2 \ll 1$ characterizing steepness, and we introduce the scaling $x' = \varepsilon x, \eta' = \eta, \xi' = \varepsilon\xi$. Expanding $G(\eta)$ and $G_1(\eta)$, and grouping terms in powers of ε in the Hamiltonian, one finds up to order $O(1)$

$$H = \frac{1}{2}\int_{\mathbb{R}} \left[R_0(\eta)u^2 + g(\rho-\rho_1)\eta^2\right] dx + O(\varepsilon^2), \tag{44}$$

where

$$R_0(\eta) = \frac{(h+\eta)(h_1-\eta)}{\rho_1(h+\eta)+\rho(h_1-\eta)},$$

and $u = \partial_x\xi$. For convenience, we have dropped the primes in (44). The corresponding approximate equations of motion are given by

$$\begin{aligned} \partial_t\eta &= -\partial_x\delta_u H = -\partial_x(R_0 u), \\ \partial_t u &= -\partial_x\delta_\eta H = -\partial_x\left[\frac{1}{2}(\partial_\eta R_0)u^2 + g(\rho-\rho_1)\eta\right]. \end{aligned} \tag{45}$$

Note that the factor $R_0(\eta)$ is nonsingular in the whole domain $-h < \eta < h_1$, vanishing at both endpoints $\eta = -h$ and $\eta = h_1$. In the case $\rho_1 = 0$, the canonical variables are $\eta(x)$ and $\xi(x) = \rho\Phi(x)$, and the equations of motion (45) reduce to

$$\partial_t\eta = -\frac{1}{\rho}\partial_x\left((h+\eta)u\right), \quad \partial_t u = -\frac{1}{\rho}u\partial_x u - g\rho\partial_x\eta, \tag{46}$$

which are the classical shallow water equations for surface water waves.

The next approximation can be derived in a straightforward

manner. Retaining terms up to order $O(\varepsilon^2)$, one gets

$$H = \frac{1}{2}\int_{\mathbb{R}} R_0(\eta)u^2 + g(\rho-\rho_1)\eta^2 + \varepsilon^2\left[R_1(\eta)(\partial_x u)^2 + (\partial_x R_2(\eta))\partial_x(u^2) + R_3(\eta)(\partial_x\eta)^2u^2\right]dx + O(\varepsilon^4). \tag{47}$$

The corresponding equations of motion read

$$\begin{aligned}
\partial_t\eta &= -\partial_x(R_0u) - \varepsilon^2\partial_x\left[-\partial_x(R_1\partial_x u) - \partial_x^2(R_2)u + R_3(\partial_x\eta)^2u\right],\\
\partial_t u &= -\partial_x\left[\frac{1}{2}(\partial_\eta R_0)u^2 + g(\rho-\rho_1)\eta\right]\\
&\quad -\varepsilon^2\partial_x\left[\frac{1}{2}(\partial_\eta R_1)(\partial_x u)^2 - \frac{1}{2}(\partial_\eta R_2)\partial_x^2(u^2) + \frac{1}{2}(\partial_\eta R_3)(\partial_x\eta)^2u^2 - \partial_x\left(R_3(\partial_x\eta)u^2\right)\right],
\end{aligned} \tag{48}$$

where

$$\begin{aligned}
R_1(\eta) &= -\frac{1}{3}\frac{(h+\eta)^2(h_1-\eta)^2(\rho_1(h_1-\eta)+\rho(h+\eta))}{(\rho_1(h+\eta)+\rho(h_1-\eta))^2},\\
\partial_x R_2(\eta) &= -\frac{1}{3}\rho\rho_1(h+h_1)(h+\eta)(h_1-\eta)\\
&\quad\times\frac{(h_1-\eta)^2-(h+\eta)^2}{(\rho_1(h+\eta)+\rho(h_1-\eta))^3}\partial_x\eta,\\
R_3(\eta) &= -\frac{1}{3}\rho\rho_1(h+h_1)^2\frac{\rho_1(h+\eta)^3+\rho(h_1-\eta)^3}{(\rho_1(h+\eta)+\rho(h_1-\eta))^4}.
\end{aligned}$$

These are novel evolution equations which exhibit nonlinear variations in wave speed and in their coefficients of dispersion. Using a different formulation and a different method, Choi and Camassa [1] also derived model equations with rational coefficients which have some similarities with (48), for large amplitude long internal waves in the configuration of two finite layers. The three-term expansion of (48) in small amplitudes (η,u), when additionally one specializes to the case of uni-directional wave motions, bears some resemblance to the extended Korteweg–de Vries equation. There is a well-known singularity of the small amplitude/long wave limit in two-layer flows, having to do with the vanishing of the coefficient of nonlinearity when $\rho/h^2 = \rho_1/h_1^2$. Our rational coefficients for the nonlinearity include this case, in which the first Taylor coefficient of the nonlinear term vanishes.

In the limit of small amplitudes, Eqs. (48) reduce to the Kaup-Boussinesq (KB) equations

$$\begin{aligned}
\partial_t\eta &= -\partial_x\left[\frac{hh_1}{\rho_1h+\rho h_1}u + \varepsilon^2\left(\frac{1}{3}\frac{(hh_1)^2(\rho_1h_1+\rho h)}{(\rho_1h+\rho h_1)^2}\partial_x^2u + \frac{\rho h_1^2-\rho_1h^2}{(\rho_1h+\rho h_1)^2}(\eta u)\right)\right],\\
\partial_t u &= -\partial_x\left[g(\rho-\rho_1)\eta + \frac{\varepsilon^2}{2}\frac{\rho h_1^2-\rho_1h^2}{(\rho_1h+\rho h_1)^2}u^2\right],
\end{aligned} \tag{49}$$

which admit explicit solitary wave solutions of the form

$$\eta(x,t) = \frac{c}{\beta}u(x,t) - \frac{\gamma}{2\beta}u(x,t)^2, \tag{50}$$

$$u(x,t) = 2\frac{\sqrt{\alpha\beta}}{\gamma}\frac{\left(\frac{c^2}{\alpha\beta}-1\right)}{\cosh\left(\sqrt{\frac{\alpha}{\delta}\left(\frac{c^2}{\alpha\beta}-1\right)}(x-ct)\right)+\frac{c}{\sqrt{\alpha\beta}}},$$

where

$$\alpha = \frac{hh_1}{\rho_1h+\rho h_1}, \quad \beta = g(\rho-\rho_1),$$

$$\delta = \frac{1}{3}\frac{(hh_1)^2(\rho_1h_1+\rho h)}{(\rho_1h+\rho h_1)^2}, \quad \gamma = \frac{\rho h_1^2-\rho_1h^2}{(\rho_1h+\rho h_1)^2},$$

and c denotes the wave speed.

Solitary Wave Solutions

We look for solutions of (48) which are stationary in a reference frame moving at constant speed c and which decay very fast at infinity. These correspond to fixed points of $\delta(H-cI)$, where $I = \int_{\mathbb{R}}\eta u\,dx$ is the momentum of the system. We thus need to solve the following system of nonlinear, ordinary differential equations

$$\begin{aligned}
0 &= -c\eta + R_0u - (R_1u')' - (R_2)''u + R_3(\eta')^2u,\\
0 &= -cu + \frac{1}{2}(\partial_\eta R_0)u^2 + g(\rho-\rho_1)\eta + \frac{1}{2}(\partial_\eta R_1)(u')^2\\
&\quad -\frac{1}{2}(\partial_\eta R_2)(u^2)'' + \frac{1}{2}(\partial_\eta R_3)(\eta')^2u^2 - \left(R_3\eta'u^2\right)',
\end{aligned} \tag{51}$$

where the symbol $'$ stands for differentiation with respect to x in the moving reference frame. Note that $\partial_\eta R_2$ in (51) is related to $\partial_x R_2$ through the chain rule $\partial_x R_2 = \partial_\eta R_2\,\partial_x\eta$.

System (51) can be solved numerically using a pseudospectral method and assuming periodic boundary conditions in x.

Both η and u are expanded in truncated Fourier series with the same number of modes N. All operations are performed using the fast Fourier transform, which yields high accuracy at relatively low cost. We solve the resulting discretized system by an iterative procedure (Newton–Raphson's method), and the bifurcation parameter in the problem is the wave speed c. Because small-amplitude waves of the KB equations are close approximations to those of (48) in the weakly nonlinear regime, we use the KB solutions (50) as the initial guess in the iterative procedure, to find solitary wave solutions of (48). We then gradually increase the parameter c (thus increasing the wave amplitude) and repeat the procedure, using smaller-amplitude solutions as an initial guess to compute higher-amplitude solutions.

Numerical Results

Computations have been performed with a discretization $N = 1024$, for a domain of length $L/h = 50$. The domain is specified long enough to ensure that the tails of the solitary waves are rapidly decaying at its ends and that periodicity has no significant effect on the solutions. As determined by the initial guess (50), we look for solitary waves moving at speeds $c^2 > c_0^2 = \alpha\beta = ghh_1(\rho-\rho_1)/(\rho_1 h + \rho h_1)$ where c_0 denotes the linear wave speed for two-layer flows. Fig. 3 shows the computed wave profiles for $h_1/h = 1/3$ and $\rho/\rho_1 = 0.997$; the solitary waves being of depression in this case. This regime of parameters was chosen because it is representative of situations close to oceanic conditions [11]. The linear wave speed in this configuration is $c_0/\sqrt{gh} = 0.0274$ (or $c_0/\sqrt{gh_1} = 0.0475$). For comparison, solitary wave solutions of the Korteweg–de Vries (KdV) and Gardner equations [12, 13] as well as those computed by the fully nonlinear model of Grue *et al.* [14], with matching amplitudes, are also shown in the figure. The model of Grue *et al.* [14] solves the full equations for two-layer flows using a boundary integral method. The KdV equation has a family of well-known 'sech^2' solitary wave solutions. For the Gardner equation (also known as the extended KdV equation), the solitary waves (also called kink-antikink solutions) are of the form

$$\eta(x,t) = -\frac{\alpha}{\alpha_1}\frac{\nu}{2}\left[\tanh\left(\frac{x-ct}{\Delta}+\delta\right) - \tanh\left(\frac{x-ct}{\Delta}-\delta\right)\right], \tag{52}$$

where

$$\alpha = \frac{3c_1(h_1-h)}{2hh_1}, \quad c_1^2 = \frac{ghh_1(\rho-\rho_1)}{\rho(h+h_1)},$$

$$\alpha_1 = \frac{3c_1}{h^2h_1^2}\left[\frac{7}{8}(h-h_1)^2 - \frac{h^3+h_1^3}{h+h_1}\right],$$

$$\Delta^2 = -\frac{24\alpha_1\beta}{\alpha^2\nu^2}, \quad \beta = \frac{c_1 hh_1}{6},$$

$$c = c_1 - \frac{\alpha^2\nu^2}{6\alpha_1}, \quad \delta = \frac{1}{4}\ln\left(\frac{1+\nu}{1-\nu}\right),$$

and ν is a nonlinearity parameter with values $0 < \nu < 1$. Solitary waves of the Gardner equation are broader than their KdV analogues, and they become more box shaped with flat crests (table-top solutions) as the amplitude increases toward the limit $\alpha/\alpha_1 = 0.857h_1$ (hereafter we define the wave amplitude as $a = |\eta|_{\max}$).

As expected, for small amplitudes, the KdV wave profiles are close to those of (48) but the latter become significantly broader as the amplitude increases. Broad internal solitary waves have also been observed by other authors, e.g. [15, 16]. We see in Fig. 3 that the 'computed' profiles (i.e. of model (48)) are also broader than the Gardner and fully nonlinear profiles for amplitudes up to $a/h_1 \simeq 0.795$; the fully nonlinear solutions lying between the Gardner and computed ones. For $a/h_1 \simeq 0.795$, the computed, Gardner and fully nonlinear wave shapes almost coincide, especially in the lower part around the wave crest. For higher amplitudes, as $\nu \to 1$, the picture is reversed; the Gardner solitary waves flatten and become broader than the computed and fully nonlinear waves.

Similar features are observed for $h_1/h = 0.24$ and $\rho/\rho_1 = 0.977$, which was the configuration considered by Camassa et al. [17] (Fig. 4).

CONCLUSIONS

In this paper, we have derived a Hamiltonian formulation for the problem of coupled free interface and free surface wave motion, in the spirit of the Hamiltonian given by Benjamin and Bridges [2] and Craig and Groves [3] for the case of one free interface with an upper rigid lid.

We have found a number of significant differences between the two cases. Even at the level of the linear dispersion relation, the linear phase and group velocities can differ. We show that for small values of the density difference $\rho - \rho_1$, the differences are small between the rigid lid and the free surface cases. However there can be significant deviations when the difference in densities is large. The deviations are most important when the ratio h_1/h is small, as one would expect.

Using the framework of Hamiltonian perturbation theory, in the setting of a free interface between two finite layers, we have derived Hamiltonian models involving coefficients of dispersion and nonlinearity which are rational functions of the interface displacement. Solitary wave solutions of these models have been computed numerically in parameter regimes close to oceanic conditions. They are found to compare reasonably well with solutions of other existing models.

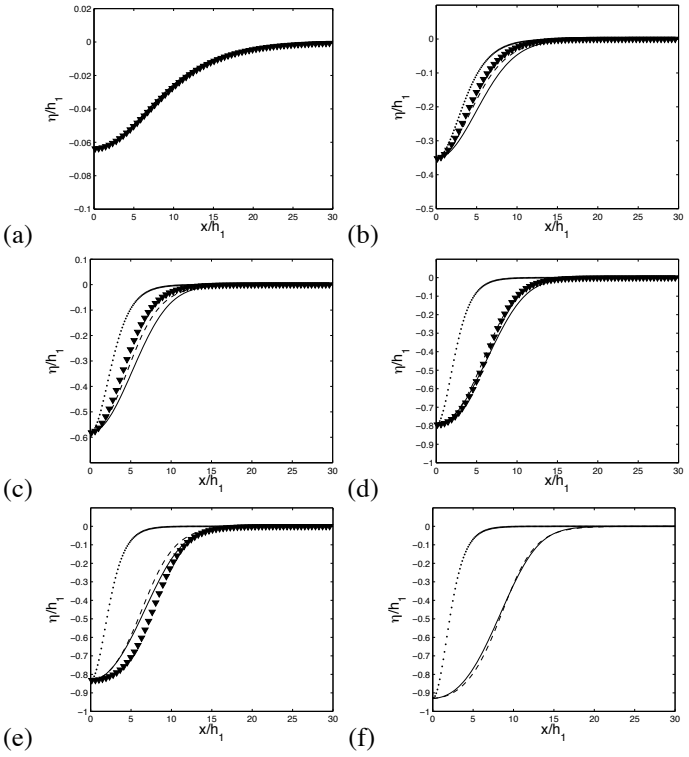

Figure 3. Comparison of wave profiles η for the KdV equation (dots), Gardner equation (triangles), fully nonlinear model of Grue *et al.* [14] (dashed line) and present model (solid line). The parameters are $h_1/h = 1/3$ and $\rho_1/\rho = 0.997$. The different plots correspond to amplitudes (a) $a/h_1 = 0.064$, (b) $a/h_1 = 0.353$, (c) $a/h_1 = 0.582$, (d) $a/h_1 = 0.795$, (e) $a/h_1 = 0.833$, (f) $a/h_1 = 0.929$.

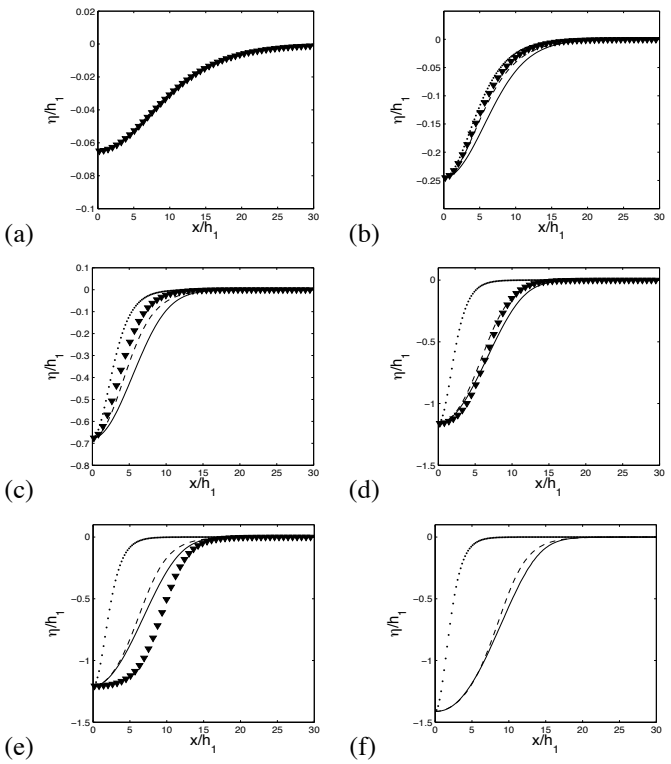

Figure 4. Comparison of wave profiles η for the KdV equation (dots), Gardner equation (triangles), fully nonlinear model of Grue *et al.* [14] (dashed line) and present model (solid line). The parameters are $h_1/h = 0.24$ and $\rho_1/\rho = 0.977$. The different plots correspond to amplitudes (a) $a/h_1 = 0.065$, (b) $a/h_1 = 0.245$, (c) $a/h_1 = 0.677$, (d) $a/h_1 = 1.161$, (e) $a/h_1 = 1.206$, (f) $a/h_1 = 1.412$.

ACKNOWLEDGMENT

P. Guyenne gratefully acknowledges support from the University of Delaware Research Foundation and the NSF through grant No. DMS-0625931. Computations of fully nonlinear solitary waves have been performed using The Internal Wave Program, developed by Per-Olav Rusås at the University of Oslo, and documented in [14].

REFERENCES

[1] Choi, W., and Camassa, R., 1999. "Fully nonlinear internal waves in a two-fluid system". *J. Fluid Mech.,* **396**, pp. 1–36.

[2] Benjamin, T., and Bridges, T., 1997. "Reappraisal of the kelvin-helmholtz problem. i. hamiltonian structure". *J. Fluid Mech.,* **333**, pp. 301–325.

[3] Craig, W., and Groves, M., 2000. "Normal forms for waves in fluid interfaces". *Wave Motion,* **31**, pp. 21–41.

[4] W. Craig, P. G., and Kalisch, H., 2004. "A new model for large amplitude long internal waves". *C. R. Mecanique,* **332**, pp. 525–530.

[5] W. Craig, P. G., and Kalisch, H., 2005. "Hamiltonian long wave expansions for free surfaces and interfaces". *Comm. Pure Appl. Math.,* **58**, pp. 1587–1641.

[6] Guyenne, P., 2006. "Large-amplitude internal solitary waves in a two-fluid model". *C. R. Mecanique,* **334**, pp. 341–346.

[7] Craig, W., and Sulem, C., 1993. "Numerical simulation of gravity waves". *J. Comp. Phys.,* **108**, pp. 73–83.

[8] Zakharov, V., 1968. "Stability of periodic waves of finite amplitude on the surface of a deep fluid". *J. Appl. Mech. Tech. Phys.,* **9**, pp. 190–194.

[9] Ambrosi, D., 2000. "Hamiltonian formulation for surface waves in a layered fluid". *Wave Motion,* **31**, pp. 71–76.

[10] Peters, A., and Stoker, J., 1960. "Solitary waves in liquids having non-constant density". *Comm. Pure Appl. Math.,* **13**, pp. 115–164.

[11] Evans, W., and Ford, M., 1996. "An integral equation ap-

proach to internal (2-layer) solitary waves". *Phys. Fluids,* **8**, pp. 2032–2047.

[12] Stanton, T., and Ostrovsky, L., 1998. "Observations of highly nonlinear internal solitons over the continental shelf". *Geophys. Res. Lett.,* **25**, pp. 2696–2698.

[13] R. Grimshaw, D. Pelinovsky, E. P., and Slunyaev, A., 2002. "Generation of large-amplitude solitons in the extended korteweg-de vries equation". *Chaos,* **12**, pp. 1070–1076.

[14] J. Grue, A. Jensen, P.-O. R., and Sveen, J., 1999. "Properties of large-amplitude internal waves". *J. Fluid Mech.,* **380**, pp. 257–278.

[15] Turner, R., and Vanden-Broeck, J.-M., 1988. "Broadening of interfacial solitary waves". *Phys. Fluids,* **31**, pp. 2486–2490.

[16] Lamb, K., and Wan, B., 1998. "Conjugate flows and flat solitary waves for a continuously stratified fluid". *Phys. Fluids,* **10**, pp. 2061–2079.

[17] R. Camassa, W. Choi, H. M. P.-O. R., and Sveen, J., 2006. "On the realm of validity of strongly nonlinear asymptotic approximations for internal waves". *J. Fluid Mech.,* **549**, pp. 1–23.